Anisotropic Mass-Spring Method Accurately Simulates Mitral Valve Closure from Image-Based Models

Peter E. Hammer[1,2,3], Pedro J. del Nido[1], and Robert D. Howe[2]

[1] Department of Cardiac Surgery, Children's Hospital Boston, MA 02115, USA
[2] Harvard School of Engineering and Applied Sciences, Cambridge, MA 02138, USA
[3] Department of Biomedical Engineering, Tufts University, Medford, MA 02155, USA
peter.hammer@childrens.harvard.edu

Abstract. Heart valves are functionally complex, making surgical repair difficult. Simulation-based surgical planning could facilitate repair, but current finite element studies are prohibitively slow for rapid, clinically-oriented simulations. An anisotropic, nonlinear mass-spring (M-S) model is used to approximate the behavior of valve leaflets and applied to fully image-based mitral valve models to simulate valve closure for fast applications like intraoperative surgical planning. This approach is used to simulate a technique used in valve repair and to assess the role of chordae in determining the closed configuration of the valve. Direct image-based comparison is used for validation. Results of M-S model simulations showed that it is possible to build fully image-based models of the mitral valve and to rapidly simulate closure with sub-millimeter accuracy. Chordae, which are presently difficult to image, are shown to be strong determinants of closed valve shape.

Keywords: Mitral valve, chordae, simulation, surgical planning, mass-spring.

1 Introduction

Surgical repair of the mitral valve is technically difficult and outcomes are highly dependent upon the experience of the surgeon [1]. One of the main difficulties of valve repair is that valve tissues must be surgically altered during open heart surgery such that the valve opens and closes effectively after the heart is closed and blood flow is restored. In order to do this successfully, the surgeon must essentially predict the displacement and deformation of anatomically and biomechanically complex valve leaflets and supporting structures. A computer-based surgical planning system could inform this task by extracting valve anatomy from pre- or intra-operative medical images and using it to create a computational mesh. This mesh could then be modified by the surgeon through a graphical interface to evaluate potential surgical repair strategies. Adequacy of a given surgical repair option could then be assessed by using computational modeling methods to simulate the opening and closing of the valve.

There have been many computational modeling studies of the mitral valve; for a review, see [2]. Most of these studies use generic models of valve anatomy to study normal or diseased valves or to assess generalized, rather than patient-specific, repair strategies. Two recent studies produced models directly from medical images [3, 4]. However, chordae could not be resolved and were modeled generically. With regard

to computation time, no previous mitral valve modeling studies have reported simulation times that are low enough for clinically practical use – on the order of a few minutes.

We present a fully image-based model of the mitral valve and use it, along with an anisotropic M-S method, to simulate the closed state of the valve under peak-systolic pressure. We use this model to simulate a simple surgical modification – replacing a chord with a suture and varying its length – and assess the accuracy of simulation results. We also use the model to predict the effect of secondary chordae on valve closure.

2   Methods

Three fresh isolated hearts from 30-40 kg female Yorkshire pigs were imaged using high resolution computed tomography (MicroCAT, Siemens, Munich, Germany). The mitral valve was loaded by delivering pressurized air to the left ventricle via tubing inserted through the aorta. Hearts were scanned with applied left ventricular pressures of 0 and 120 mmHg, producing volumetric images with isotropic voxel size of 100 μm (Fig. 1, A and B).

Images were cropped and segmented, and triangular meshes were generated using custom software based on published methods [5]. The mesh produced from the open valve was used to define the leaflet surface for simulating valve closure. Meshes were produced with 600 – 700 triangles per valve. The open valve mesh was also used to define chordae, specified by segment endpoints. The mesh produced from the pressurized valve (Fig. 1, C and D) defined the closed surface of the pressurized valve to be used for comparison with simulations of the pressurized valve. It was also used to define the annulus and papillary muscle locations to be used as boundary conditions for the simulated closure as well as to define lengths and attachment points of those chordae not visible in the image of the open valve.

Closure of the mitral valve mesh was simulated using a dynamic M-S model that has been previously described [6]. The nonlinear anisotropic behavior of the mitral valve leaflets was modeled using bilinear functions that were fit to published stress-strain relationships for mitral valve leaflet tissue [7]. One bilinear function is used for
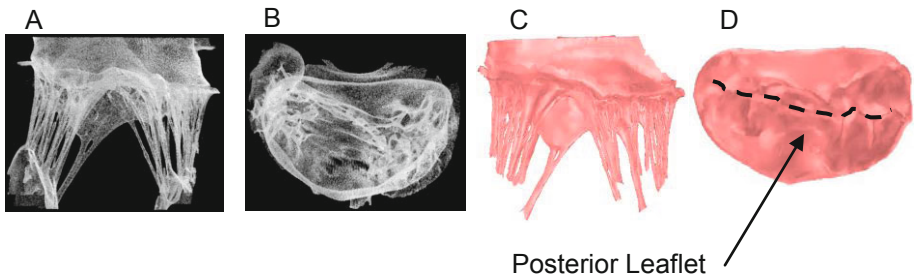

Posterior Leaflet

Fig. 1. Volume rendered micro-CT scan of valve 3 under 120 mmHg of pressure, shown from side view (*A*) and top view (*B*). Surface rendered mesh produced directly from CT scan data of same valve are shown in side view (*C*) and top view (*D*) with portion of mesh beyond the annulus trimmed and coaptation line highlighted (*dotted line*).

the preferential fiber direction (circumferential direction in the leaflet), and another is used for the cross-fiber direction (radial direction in the leaflet). Chordae are modeled as linear elastic rods with constant diameter supporting tension only, with Young's modulus taken from published data [8].

Dynamic simulation consists of two parts. First, mesh nodes lying on the valve annulus are forced to their positions on the closed mesh while points of chordae attachment to the papillary muscles are held fixed. Next, leaflet annulus nodes are also held fixed while force due to pressure (120 mmHg) is applied to the ventricular surface of all mesh triangles. Semi-implicit numerical integration with adaptive time step control was used to solve the equations of motion, and self-contact of leaflets was handled using a fast sort of axis-aligned bounding boxes of mesh triangles to screen for potential triangle collisions followed by triangle-to-triangle intersection checking [6]. Collisions were resolved using a linear penalty force set to balance the net external force bringing the triangles together, resulting in frictionless contact.

One of the hearts was used in an experiment in which a posterior leaflet primary chord was transected and replaced with a suture. The suture was brought through the papillary muscle and LV wall so that its length could be varied. While applying pressure to the LV, the chord was pulled (shortened) as far as possible without causing a leak, then a CT scan of the heart was taken and subsequently meshed (Fig. 2). This chord shortening procedure was simulated by changing the resting length of the corresponding posterior leaflet primary chord of the open valve mesh and simulating valve closure.

The closed valve meshes produced by simulation were compared with the meshes produced directly from images of the closed valve by registering the surfaces and computing surface-to-surface error as the distance from each node on the simulated closed mesh to the nearest node on the mesh from the image of the closed valve.
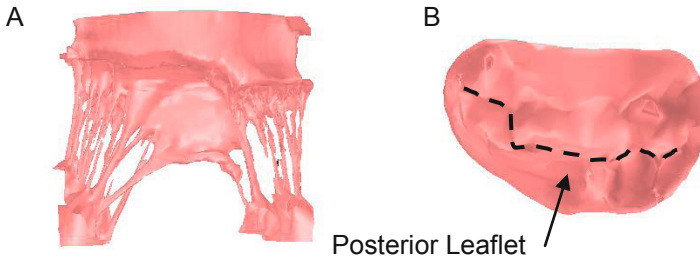

Fig. 2. Surface rendering of a mesh produced from a micro-CT scan of valve 3 under 120 mmHg of pressure and with one posterior leaflet chord replaced with suture. Mesh is shown from side (*A*) and top views (*B*), with coaptation line highlighted (*dashed line*).

3   Results

Valve closure and loading was simulated in less than 25 seconds, on a 2.3 GHz CPU utilizing a single core, for each of the three valves. Image-based validation resulted in mean surface-to-surface error of approximately 0.8 mm for all three valves (Table 1). The maximum surface-to-surface error was 2.4 to 3.0 mm and typically occurred near the line of coaptation as seen in the error maps (Fig. 3). Simulations in which a

posterior leaflet primary chord was shortened resulted in restricted movement of that portion of the posterior leaflet, and the opposing (anterior) leaflet moved to fill the gap. Mean and maximum surface-to-surface error magnitudes were 1.1 and 3.3 mm, respectively (Table 1 and Fig. 4, B).

Simulations of the three valves were repeated with all secondary chordae omitted, and mean and maximum surface-to-surface errors increased more than two-fold (Table 1, rows 1 – 3, last column). Absence of secondary chordae resulted in peak values of surface-to-surface error occurring near the center of the anterior leaflet (Fig. 5), reaching values of approximately 7 mm.

Sensitivity analysis was conducted for model parameters affecting mesh geometry or material properties. Each parameter was subject to +/- 5% perturbation, and the changes in the mean surface-to-surface error magnitude of the resulting simulations were measured. Of the ten parameters that were examined (six parameters of the constitutive law bilinear functions, chordae diameter, chordae stiffness, chordae rest length, and leaflet thickness), only chordae rest length and the two constitutive law parameters controlling the breakpoints of the bilinear functions exhibited sensitivity of greater than 1mm of error per 100% change in parameter. Resting chord length exhibited the highest sensitivity, with a value of approximately 8mm per 100% change.

Table 1. Number of triangles, nodes and chord segments comprising the valve models, along with simulation time and mean & maximum errors in the closed state for simulations with all chordae and with primary chordae only. Row 4 corresponds to a simulation with valve #3 incorporating a shortened chord (sc). Rows 5 and 6 correspond to simulations with valve #3 where the mesh was upsampled by four (x4) and sixteen (x16), respectively.

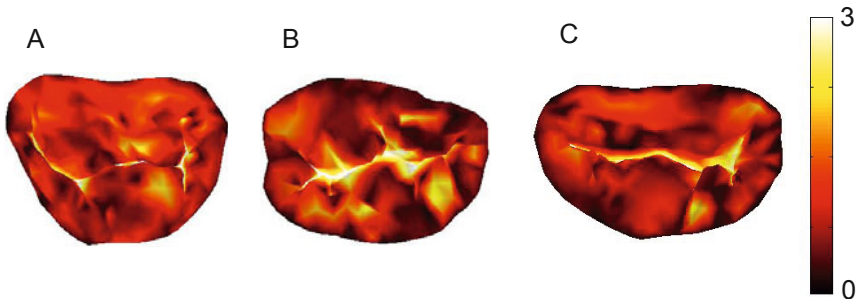| valve I.D.	# of triangles	# of nodes	# of chords	time (sec)	e_{all} (mm) mean, max	e_{pri} (mm) mean, max
1	655	414	52	21.4	0.8, 2.4	1.9, 7.4
2	621	406	53	20.0	0.8, 3.0	2.0, 7.2
3	624	425	77	24.8	0.8, 2.5	1.8, 6.4
3_{sc}	624	425	77	22.9	1.1, 3.3	-
3_{x4}	2,496	1,423	77	103	0.9, 2.9	-
3_{x16}	9,984	5,291	77	1240	0.9, 2.7	-

Fig. 3. Magnitude of error, expressed as distance in mm, between closed valve surface predicted by simulation and closed valve surface from image, for valves 1 – 3 are shown in (A) – (C), respectively. Simulations were run with all (both primary and secondary) chordae.
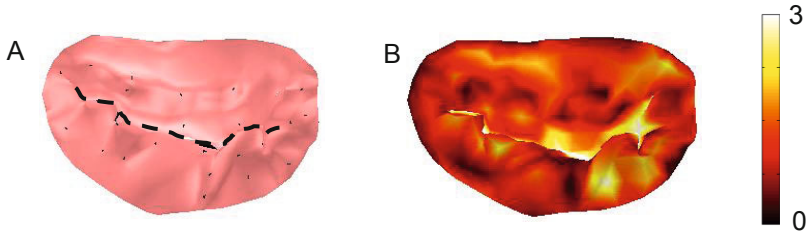
Fig. 4. Top view of mesh of valve 3 produced by simulating valve closure after simulated chord shortening (*A*). Coaptation line is highlighted (*dashed line*). Magnitude of error, expressed as distance in mm, between closed mesh produced by simulation and mesh produced directly from closed image (*B*).
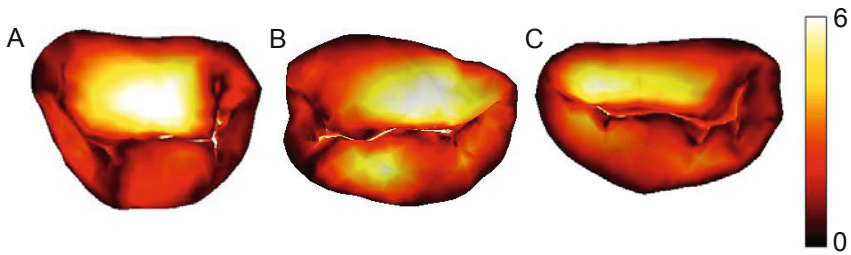

Fig. 5. Magnitude of error, expressed as distance in mm, between closed valve surface predicted by simulation and closed valve surface from image, for valves 1 – 3 are shown in *(A)* – *(C)*, respectively. Simulations were run with primary chordae only. Note change of scale compared to Figs. 3 and 4.
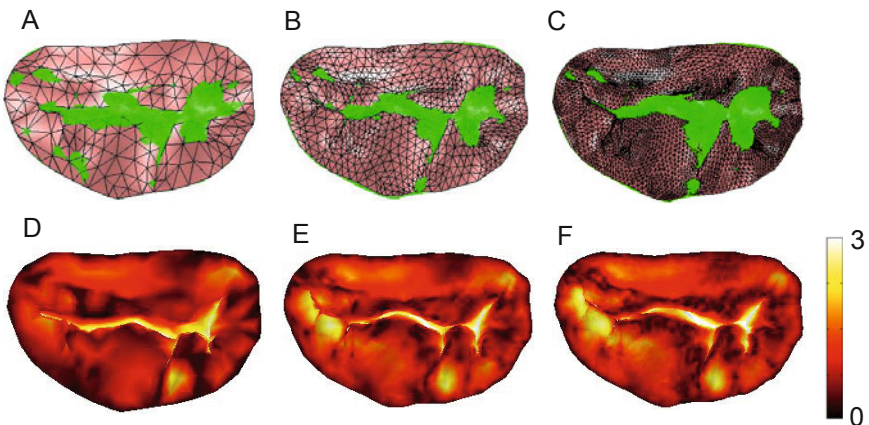

Fig. 6. Meshes of valve 3 in the closed state (*pink*) are superimposed on the mesh produced from the image of closed valve surface, shown in green with triangle edges hidden (*A, B,* and *C*). Surface-to-surface error in mm is mapped onto the closed mesh from simulation (*D, E,* and *F*). Meshes contain approximately 625 (*A, D*), 2500 (*B, E*), and 10000 (*C, F*) triangles.

The effect of mesh size on simulation accuracy was assessed by subdividing the triangles of valve 3 by factors of 4 and 16 and simulating closure. The mean and maximum errors for the simulated meshes did not change significantly in response to either of the two increased mesh sizes (Table 1 and Fig. 6).

4   Discussion

The aim of this study was to develop a method for producing fast, image-based simulations of mitral valve closure for use in planning surgical repair. We showed that it was possible to take an image of a mitral valve and from it develop a model that could be used to quickly and accurately predict closure and loading of the valve. Furthermore it was shown that the method could successfully predict the effect of a surgical repair technique.

A major requirement guiding the development of the simulation methods was that the closed and loaded state of the valve be computed quickly through judicious use of approximation. For the three mitral valve specimens simulated in this study, the closed, loaded state was computed in less than 30 seconds using an anisotropic M-S model, efficient contact handling and bilinear approximation of published material constitutive laws. While the M-S method gains much of its speed advantage by neglecting to adhere to a continuum description of the tissue, image-based validation showed that accuracy of prediction of the closed state is high. Another significant approximation is the use of relatively coarse meshes. However, increasing the number of triangular faces in the mesh did not improve the overall accuracy with which the simulated closed surface approximated the actual closed valve surface. Increasing mesh size marginally improved mesh closure near the coaptation line. On the other hand, it also led to slight error increases in leaflet regions untethered by chordae, because the new nodes of the subdivided triangles are not constrained by chordae and consequently displace in the direction of the applied pressure.

A second requirement guiding the development of simulation methods was that model geometry be based directly on images of the valve. Only two groups have published mitral valve models that incorporate image-based models of the leaflets, but neither was able to resolve chordae [3], [4]. We chose to use an experimental imaging method – micro-CT and pressurization with air – rather than a clinically applicable method in order to develop highly detailed geometric models that make it possible to assess the importance of various aspects of model detail for accurate valve simulation. Results of omitting secondary chordae and of the sensitivity analysis suggest that details of the chordae network are important determinants of the closed valve state. One of the published studies using image-based leaflet models used image-based validation and found an average discrepancy between closed models and images of closed valves of four to five mm [3]. Their levels of mean error are five to six times higher than those achieved in our study. This is probably due in part to the lower intrinsic resolution to their imaging modality, but their neglect of secondary chordae, which we have shown to strongly influence closed valve shape, likely played a significant role.

Although our study uses dynamic simulation, only a single state of the valve cycle – peak systolic pressure load – is used to assess whether a valve leaks. One justification for this is that the transvalvular gradient at peak systole represents the

greatest mechanical challenge to valve structures and a worst-case scenario for inducing a leak. An additional, more clinical justification is that surgeons test the repaired valve in a similar way by injecting saline under static pressure into the LV [9]. The assumption that it is sufficient to assess valve function at peak systolic pressure allows the complex interaction between blood flow and the valve structures during ventricular filling and ejection to be neglected. Another limitation of this study is that models were produced from porcine rather than human valves, however anatomical studies have shown that valve leaflet dimensions and chord lengths are not significantly different between human and porcine valves [10].

5   Conclusion

We have shown that it is possible to take image-based mitral valve models and use simulation to rapidly and accurately predict the closed valve shape and the effects of surgical manipulation. The remaining challenge is to build the valve models from clinically relevant imaging. A recent study has shown that the mitral valve leaflets and annulus can be extracted from 3D ultrasound images [11]. Using clinical imaging to resolve the chordae, which we have shown to be critical for predicting the closed shape of the valve, has yet to be solved.

References

[1] Vahanian, A., Baumgartner, H., Bax, J., Butchart, E., Dion, R., Filippatos, G., Flachskampf, F., Hall, R., Iung, B., Kasprzak, J., Nataf, P., Tornos, P., Torracca, L., Wenink, A.: Grupo de Trabajo sobre el Tratamiento de las Valvulopatias de la Sociedad Europea de Cardiologia: Guidelines on the management of valvular heart disease. Rev. Esp. Cardiol. 60, 1e–50e (2007)

[2] Kunzelman, K.S., Einstein, D.R., Cochran, R.P.: Fluid-structure interaction models of the mitral valve: function in normal and pathological states. Philos. Trans. R. Soc. Lond. B. Biol. Sci. 362, 1393–1406 (2007)

[3] Burlina, P., Sprouse, C., DeMenthon, D., Jorstad, A., Juang, R., Contijoch, F., Abraham, T., Yuh, D., McVeigh, E.: Patient-specific modeling and analysis of the mitral valve using 3D-TEE. In: Navab, N., Jannin, P. (eds.) IPCAI 2010. LNCS, vol. 6135, pp. 135–146. Springer, Heidelberg (2010)

[4] Wenk, J.F., Zhang, Z., Cheng, G., Malhotra, D., Acevedo-Bolton, G., Burger, M., Suzuki, T., Saloner, D.A., Wallace, A.W., Guccione, J.M., Ratcliffe, M.B.: First finite element model of the left ventricle with mitral valve: insights into ischemic mitral regurgitation. Ann. Thorac. Surg. 89, 1546–1553 (2010)

[5] Persson, P.-O., Strang, G.: A Simple Mesh Generator in MATLAB. SIAM Review 46, 329–345 (2004)

[6] Hammer, P.E., Sacks, M.S., del Nido, P.J., Howe, R.D.: Mass-spring model for simulation of heart valve tissue mechanical behavior. Ann. Biomed. Eng. (2011) (in press)

[7] Sacks, M.S., Yoganathan, A.P.: Heart valve function: a biomechanical perspective. Philos. Trans. R. Soc. Lond. B. Biol. Sci. 362, 1369–1391 (2007)

[8] Kunzelman, K.S., Cochran, R.P., Chuong, C., Ring, W.S., Verrier, E.D., Eberhart, R.D.: Finite element analysis of the mitral valve. J. Heart Valve Dis. 2, 326–340 (1993)

[9] Cohn, L.H. (ed.): Cardiac Surgery in the Adult. McGraw-Hill, New York (2008)

[10] Kunzelman, K.S., Cochran, R.P., Verrier, E.D., Eberhart, R.C.: Anatomic basis for mitral valve modelling. J. Heart Valve Dis. 3, 491–496 (1994)

[11] Schneider, R.J., Perrin, D.P., Vasilyev, N.V., Marx, G.R., del Nido, P.J., Howe, R.D.: Mitral annulus segmentation from 3D ultrasound using graph cuts. IEEE Trans. Med. Imaging 29, 1676–1687 (2010)